Evoked Effective Connectivity of the Human Neocortex

László Entz,[1,2,3,4] Emília Tóth,[2,3,4] Corey J. Keller,[1,5] Stephan Bickel,[1,6] David M. Groppe,[1] Dániel Fabó,[3,4] Lajos R. Kozák,[7] Loránd Erőss,[3,4] István Ulbert,[2,3,4] and Ashesh D. Mehta[1]*

[1]*Department of Neurosurgery, Hofstra North Shore LIJ School of Medicine and Feinstein Institute of Medical Research, Manhasset, New York 11030*
[2]*Institute of Cognitive Neuroscience and Psychology, Research Centre for Natural Sciences, Hungarian Academy of Sciences, Budapest, 1132, Hungary*
[3]*Department of Functional Neurosurgery and Department of Epilepsy, National Institute of Clinical Neuroscience, Budapest, 1145, Hungary*
[4]*Péter Pázmány Catholic University, Faculty of Information Technology and Bionics, Budapest, 1083, Hungary*
[5]*Department of Neuroscience, Albert Einstein College of Medicine, Bronx, New York, 10461*
[6]*Department of Neurology, Albert Einstein College of Medicine, Bronx, New York, 10461*
[7]*MR Research Center, Semmelweis University Budapest, 1083, Hungary*

◆ ════════════════════ ◆

Abstract: The role of cortical connectivity in brain function and pathology is increasingly being recognized. While in vivo magnetic resonance imaging studies have provided important insights into anatomical and functional connectivity, these methodologies are limited in their ability to detect electrophysiological activity and the causal relationships that underlie effective connectivity. Here, we describe results of cortico-cortical evoked potential (CCEP) mapping using single pulse electrical stimulation in 25 patients undergoing seizure monitoring with subdural electrode arrays. Mapping was performed by stimulating adjacent electrode pairs and recording CCEPs from the remainder of the electrode array. CCEPs reliably revealed functional networks and showed an inverse relationship to distance between sites. Coregistration to Brodmann areas (BA) permitted group analysis. Connections were frequently directional with 43% of early responses and 50% of late responses of connections reflecting relative dominance of incoming or outgoing connections. The most consistent connections were seen as outgoing from motor cortex, BA6–BA9, somatosensory (SS) cortex, anterior cingulate cortex, and Broca's area. Network topology revealed motor, SS, and premotor cortices along with BA9 and BA10 and

language areas to serve as hubs for cortical connections. BA20 and BA39 demonstrated the most consistent dominance of outdegree connections, while BA5, BA7, auditory cortex, and anterior cingulum demonstrated relatively greater indegree. This multicenter, large-scale, directional study of local and long-range cortical connectivity using direct recordings from awake, humans will aid the interpretation of noninvasive functional connectome studies. *Hum Brain Mapp 35:5736–5753, 2014.* © 2014 **Wiley Periodicals, Inc.**

Key words: cortical stimulation; effective connectivity; epilepsy; evoked potentials; Brodmann's areas

INTRODUCTION

The human brain connectome may be described by three forms of connectivity: anatomical, functional, and effective [Rubinov and Sporns, 2010]. Anatomical connectivity describes the anatomical links indicated by tracer and magnetic resonance imaging (MRI) tractography [Conturo et al., 1999; Felleman and Van Essen, 1991; Hagmann et al., 2008], while functional connectivity is typically measured by statistical dependencies in the blood oxygen level-dependent signal and the electrocorticogram [Fox et al., 2005; Keller et al., 2013; Vincent et al., 2007]. However, these measures do not assess relationships of causal influence that one brain area may have over another. Quantifications of this influential relationship, termed effective connectivity, are more difficult to study. Prior attempts have relied on Granger causality [Brovelli et al., 2004] and dynamic causal modeling [Friston et al., 2003; McIntosh and Gonzalez-Lima, 1994]. However, these observational methods rely on statistical covariance [Smith et al., 2011] as opposed to interventional empiric testing. Combining transcranial magnetic stimulation (TMS) with electroencephalography (EEG), magnetoencephalography (MEG), or functional MRI (fMRI) provides a more empiric effective connectivity assessment [Massimini et al., 2005], but this method also has limitations related to the difficulty of inferring intracranial neural measurements from extracranial stimulation using assumptions of EEG/MEG source modeling or indirect measures of neural activity with fMRI.

Epilepsy patients undergoing surgical evaluation provide an opportunity to directly record human brain electrophysiology with high spatiotemporal resolution. In these subjects, effective connectivity may be assessed empirically by applying single pulses of electrical current at one cortical region and recording the cortico-cortical evoked potential (CCEP) at other remote locations [Catenoix et al., 2005, 2011; David et al., 2013; Enatsu et al., 2013; Lacruz et al., 2007; Matsumoto et al., 2004, 2007, 2012; Valentin et al., 2002, 2005; Yamao et al., 2014]. CCEP mapping typically does not elicit the behavioral effects that are observed with clinical electrical stimulation mapping (ESM; 20–50 Hz stimulation, 1–15 mA amplitude, 0.2–0.5 ms pulse width, and 1–3 s duration) protocols to map eloquent cortical areas [Gordon et al., 1990; Hamberger, 2007]. Instead, field potentials evoked by single pulse electrical stimulation (SPES) can be averaged to compute a CCEP profile over the remainder of implanted electrodes. CCEPs consist of an initial early (10–50 ms) biphasic N1, and a delayed (50–500 ms), slow N2 wave [Creutzfeldt et al., 1966; Lacruz et al., 2007]. The N1 is thought to reflect direct activation of the local cortex [Goldring et al., 1994; Matsumoto et al., 2004; Purpura et al., 1957], while the N2 may represent a later inhibition [Creutzfeldt et al., 1966; Entz et al., 2009], similar to spontaneously recorded and induced human slow oscillations generated by cortical and subcortical (thalamic) interactions [Cash et al., 2009; Catenoix et al., 2011; Csercsa et al., 2010; Hangya et al., 2011; Logothetis et al., 2010; Matsumoto et al., 2004; Rosenberg et al., 2009; Steriade, 2003].

As both N1 and N2 responses have been shown to be predicted by resting functional connectivity measures using fMRI [Keller et al., 2011], we examined both CCEP components to assess correspondence and consistency. To account for intersubject variability in electrode placement, in this report, we map intracranial electrodes to a modified parcellation scheme based on Brodmann areas (BAs) defined by Montreal Neurological Institute (MNI) space. This permitted us to combine results across 25 subjects at two different institutions to present a more comprehensive CCEP-based effective connectivity map of the human neocortex. Our results demonstrate both a consistency of certain connections as well as the fact that many connections are directed.

MATERIALS AND METHODS

Patient Selection

Twenty-five patients (14 female) with medically refractory epilepsy were enrolled at the Comprehensive Epilepsy Center at North Shore University Hospital (Manhasset, NY), Long Island Jewish Medical Center (New Hyde Park, NY—NSLIJ), and the National Institute of Clinical Neuroscience (Budapest, Hungary—NIN). Patients participating in this study had medically intractable seizures and were referred for epilepsy surgical evaluation. All patients underwent intracranial electrode implantation for localization of epileptogenic tissue. Patient demographics are depicted in Table I. All patients provided informed consent along institutional review board guidelines, according to the Declaration of Helsinki.

Electrode Implantation

Following noninvasive presurgical evaluation, patients underwent subdural strip, grid and depth electrode

TABLE I. Patient demographics

No.	MRI finding	Age at implantation	Seizure frequency per month	Surgery performed	Brodmann's areas covered with electrodes	Number of electrodes
P1	Normal	22	14	R-AH	$N = 20$ (BA: 1, 2, 3, 4, 6, 8, 9, 10, 11, 20, 21, 22, 24, 31, 35, 37, 39, 42, 44, 46)	112
P2	R temporal lobe encephalomalacia	47	1	R-AHTL	$N = 14$ (BA: 2, 3, 4, 9, 10, 20, 21, 37, 39, 42, 43, 44, 45, 46)	74
P3	Normal	48	8	R-AH	$N = 14$ (BA: 1, 2, 3, 4, 6, 8, 9, 19, 41, 42, 43, 44, 45, 46)	86
P4	R temporo-polar dysgenesis	35	30	None	$N = 3$ (BA: 22, 38, 44)	23
P5	L occipito-temporal dysplasia	23	30	L-occipito-temporal topectomy	$N = 19$ (BA: 1, 2, 3, 4, 6, 7, 8, 9, 10, 11, 21, 22, 34, 38, 39, 40, 42, 43, 45)	110
P6	L temporal encephalomalacia	55	6	L-temporal lateral lesionectomy	$N = 17$ (BA: 1, 2, 4, 6, 8, 9, 10, 11, 19, 20, 40, 41, 42, 44, 45, 46, 47)	81
P7	Normal	36	1	None	$N = 10$ (BA: 3, 6, 9, 18, 37, 38, 43, 44, 45, 46)	95
P8	L frontal tumor	38	1.5	L-frontal lesionectomy	$N = 10$ (BA: 5, 7, 9, 10, 21, 22, 40, 42, 44, 46	66
P9	R cingular and frontal CD	20	6	R-frontal topectomy	$N = 2$ (BA: 10, 44)	33
P10	R frontal encephalomalacia	18	10	R-frontal lesionectomy	$N = 7$ (BA: 3, 4, 6, 7, 8, 10, 46)	29
P11	L temporal arachnoid cyst	60	10	L-temporal lateral topectomy	$N = 19$ (BA: 1, 2, 3, 4, 5, 6, 7, 9, 10, 11, 37, 39, 40, 42, 43, 44, 45, 46, 47	97
P12	R multiple gangliogliomas	25	1.5	R-multiple lesionectomies	$N = 14$ (BA: 2, 3, 4, 5, 6, 9, 17, 18, 19, 22, 29, 31, 39, 42)	100
P13	Normal	15	8	None	$N = 17$ (BA: 2, 4, 6, 8, 9, 10, 11, 19, 20, 28, 37, 38, 39, 44, 45, 46, 47)	113
P14	R occipito-temporal encephalomalacia	31	2.5	R-AHTL	$N = 10$ (BA: 1, 2, 3, 4, 7, 11, 42, 44, 45, 47)	79
P15	Normal	30	0.5	R-temporo-parietal junction and insular topectomy	$N = 16$ (BA: 6, 7, 8, 9, 10, 11, 18, 19, 20, 21, 37, 38, 39, 44, 45, 46)	105
P16	Normal	26	30	L-temporal and orbitofrontal topectomy	$N = 16$ (BA: 1, 2, 3, 4, 6, 7, 9, 10, 19, 35, 36, 37, 39, 40, 43, 46)	101
P17	R occipito-temporal encephalomalacia	32	30	R-occipital topectomy and R-AH	$N = 5$ (3, 4, 5, 6, 20)	27
P18	Normal	23	0.5	L-AHTL	$N = 13$ (BA: 3, 4, 6, 8, 9, 10, 22, 25, 32, 40, 44, 45, 46)	95
P19	R occipito-parieto-temporal dysplasia	17	4	R-temporo-parietal topectomy	$N = 15$ (BA: 2, 4, 5, 6, 7, 10, 11, 21, 22, 39, 40, 41, 43, 46, 47)	91
P20	Normal	30	2	None	$N = 8$ (BA: 2, 5, 6, 7, 8, 9, 10, 46)	55
P21	L occipito-temporal dysgenesis	17	12	L-occipito-polar topectomy	$N = 6$ (BA: 28, 29, 30, 31, 35, 42)	38
P22	Normal	40	14	L-AH	$N = 21$ (BA: 1, 2, 3, 4, 6, 7, 8, 9, 10, 18, 19, 21, 22, 28, 32, 37, 40, 42, 43, 44, 46)	99
P23	L hippocampal sclerosis	36	16	L-AH	$N = 16$ (BA: 2, 4, 6, 9, 10, 11, 25, 30, 37, 38, 40, 42, 44, 45, 46, 47)	92
P24	L frontal opercular— insular dysgenesis	29	90	L frontal–opercular topectomy	$N = 12$ (BA: 8, 9, 20, 21, 22, 27, 38, 40, 41, 45, 46, 47)	39
P25	R temporal CD	37	4	R temporal topectomy	$N = 9$ (BA: 1, 2, 3, 20, 36, 38, 42, 43, 44)	38

Twenty-five patients were enrolled at two different epilepsy surgical centers. MRI finding, age at implantation surgery, resection type, covered Brodmann's areas and nonictal electrode numbers in each patient are shown.

CD, cortical dysplasia; AH, amygdalo-hyppocampectomy; AHTL, amygdalo-hyppocampectomy with anterior temporal lobe resection; R, right side; L, left side.

implantation (NSLIJ: Integra Lifesciences Corp., Plainsboro, New Jersey, NIN: AD TECH Medical Instrument Corp., Racine, WI). Subdural electrodes (10 mm intercontact spacing) were implanted with the aid of neuronavigation and fluoroscopy to maximize accuracy [Eross et al., 2009] via craniotomy with targets defined by clinical grounds. Video-EEG monitoring was performed using Xltek EMU 128 LTM System (San Carlos, CA) at NSLIJ and a Brain Quick System 98 (Micromed, Mogliano Veneto, Italy) at NIN. All signals were recorded with reference to the skull or mastoid at a 1 or 2 kHz sampling rate.

3D Electrode Reconstruction and BA Colocalization

To identify the electrode locations, all participants received an anatomical T1-weighted MRI before electrode implantation as well as a full head CT scan and an anatomical T1-weighted MRI after electrode implantation. Pre-implantation MRIs were performed on a General Electric Signa HDx 3T scanner using one of two spoiled gradient recalled sequences (field of view [FOV] = 256 or 240 mm, voxel size $1 \times 1 \times 1$ or $1.2 \times 0.9 \times 0.9$, matrix 256×256, pulse repetition time [TR] = 7.8 or 6.5 ms, echo time [TE] = 3.0 or 2.8 ms, acquisition plane = axial or saggital, slices = 180 or 170) or on a Philips Achieva 3T scanner using Turbo Field Echo (equivalent of spoiled gradient echo) sequences [FOV = 240 mm, voxel size $1 \times 1 \times 1$, matrix 240×240, TR: 9.8 ms, TE: 4.6ms, acquisition plane = saggital, slices = 180]. Postimplantation volumetric MRIs were performed on 1.5T scanner using standard clinical protocols.

Electrode locations were identified on the postimplantation CT scan using the software BioImage Suite [http://www.bioimagesuite.org; Duncan et al., 2004]. These locations were then mapped to the preimplant MRI via an affine transformation derived from coregistering the pre-implant and postimplant MRIs and postimplant MRI and CT scans using FLIRT [Jenkinson and Smith, 2001] and the skull-stripping BET 2 algorithm [Smith, 2002], both part of the Oxford Centre for Functional MRI of the Brain (FMRIB) software library (FSL: www.fmrib.ox.ac.uk/fsl). The reconstructed pial surface was computed from the preimplantation MRI using FreeSurfer [http://surfer.-nmr.mgh.harvard.edu/; Dale et al., 1999] and the electrode coordinates projected to the pial surface [Dykstra et al., 2011] to correct for possible brain shift caused by electrode implantation and surgery. Intraoperative photographs and ESM were used to corroborate this registration method. This pial surface projection method has been shown to produce results that are compatible with the electrode locations in intraoperative photographs [median disagreement of ~3 mm: Dykstra et al., 2011].

Coregistering the preoperative MRI to standard MNI and Talairach space allowed the identification of the nearest BA to each electrode using AFNI (http://afni.nimh. nih.gov/). This automated process was corroborated with manual inspection of two independent researchers and compared to the ESM results to correct for individual differences from standard brain maps.

Inclusion and Exclusion Criteria for Patients and Sites

Patients with IQ less than 70 were excluded from this study due to the possible brain organizational differences compared to average IQ patients. Any electrode having fast activity coincident with seizures as well as brain regions with overt structural abnormalities were excluded from analysis. High frequency (bipolar 20–50 Hz) ESM results for motor, language and sensory mapping were used as supplemental information to assign BAs when electrodes were positioned on the border between two regions. Sensory (auditory, visual, and somatosensory [SS]), motor and language function were tested separately using clinical ESM by a neurosurgeon, neurologist, and/or neuropsychologist. For any analysis using BAs, only those stimulating electrodes lying within the same BA were included in this study. Electrodes within the same BA as the ictal onset (as determined by an epileptologist blinded to this study) were removed from analysis. Depth electrodes were excluded from analysis because their spatial configuration and penetration into the brain parenchyma could result in a different charge density, geometry, and tissue electrical resistance, which would not be comparable to the grid and strip electrode contacts.

Despite these exclusions, all BAs, except 12, 23, 25, 26, 30, 33, 48, 49, and 52 were covered with implanted electrodes. The number of electrodes per area is shown in Table II. Data from both hemispheres were combined in the group analysis, but only intrahemispheric connectivity was analyzed due to the limited number of patients with bihemispheric coverage. We computed connectivity among functional regions of the cortex by grouping BAs of similar function to increase sample size without averaging across heterogeneous anatomico-functional areas. The groups created are as follows: BA1–3: SS; BA44,45: Broca's area (BR); BA11,12,25,47: prefrontal cortex (PFC); BA23,26,29,30,31: posterior cingulate cortex (PCC); BA 24,32,33: anterior cingulate cortex (ACC); BA 34,35,36: parahippocampal gyrus (PHG); BA41,42: auditory cortex (AU). These categories were combined across hemispheres.

CCEP Mapping

For CCEP mapping, brief single current pulses were injected into all adjacent electrode contacts (10 mA, 0.2 ms pulse width, 20 trials) over the implanted array using a Grass S12 cortical stimulator (Grass Technologies Inc, West Warwick, RI) or an IRES Surgical 600 cortical stimulator (Micromed S.p.A. Via Giotto, 2–31021, Mogliano Veneto—Italy; [Matsumoto et al., 2004]). The amplitude

TABLE II. Sampling Brodmann's areas

	# of stimulating electrodes	# of patients	# of recording electrodes	# of patients
M	119	21	133	22
PM	158	22	192	23
BA8	68	15	74	15
BA9	108	19	124	21
BA10	107	18	121	20
PFC	65	16	87	17
BR	82	19	96	20
BA46	47	19	59	21
SS	110	22	124	23
BA5	7	6	10	8
BA7	34	11	54	13
BA39	30	12	32	11
BA40	125	22	133	22
BA20	108	21	131	22
BA21	151	23	158	23
BA22	133	22	150	22
BA37	74	17	83	18
BA38	96	18	121	18
AU	28	17	31	18
V1	4	2	7	2
V2	30	7	34	7
V3	73	14	82	14
BA43	10	9	13	11
BA27	1	1	1	1
BA28	7	6	8	7
PCC	8	4	17	6
ACC	12	6	12	6
PHG	39	12	50	14

Table summarizes the number of electrodes localized over each BA and the corresponding number of patients included in each region of interest. First two columns refers to the number of stimulating electrodes and patients, the third and fourth columns show the number of recording electrodes and the respective patient number.

was selected based on previous reports [Matsumoto et al., 2004, 2007] and our preliminary data showing no additional effect on the evoked response above 10 mA (Fig. 2, upper right panel). Those electrodes—selected by an epileptologist—which indicated seizure-onset or early seizure spread (first 10 s after seizure-onset) were removed from the analysis. The recorded ElectroCorticoGraphy (ECoG) sessions were visually inspected for afterdischarges and ictal events. Afterdischarges or ictal activity that were present during the stimulation period were excluded from analysis. CCEP mapping was done after the antiepileptic medication was resumed. The majority of patients (P1–P22) underwent 0.5 Hz stimulation, with a subset (P23–25) receiving 1 Hz stimulation. No obvious difference in CCEP morphology was observed between the two groups. Stimulation was performed extraoperatively at the bedside while the patient was awake and resting. Subsequently, evoked responses to stimulation were divided into 1 s epochs (200 ms prestimulation to 800 ms poststimulation). These responses were time-locked to delivery of the stimulation pulse and averaged using commercial software (Neuroscan, Compumedics, Charlotte, NC). The stimulation artifact (~5 ms) was not taken into account as the peristimulation period between −50 and +10 ms was not included in the CCEP analysis (Baseline: −200 to −50 ms, N1: 10–50 ms, N2: 50–500 ms). Evoked CCEP curves underwent artifact rejection (visual inspection and voltage threshold criteria). The averaged response was full-wave rectified (absolute value of every measured datapoint after baseline correction). A z-score of the local maximum (using the findpeaks function of Matlab/Signal Processing Toolbox) was calculated compared to prestimulus baseline changes (Fig. 2).

### Assignment of Brodmann's Area

To permit a group analysis and account for structural and functional differences between each patient's brain, we assigned a BA to each stimulating and recording site. z-scores of electrodes located within the same BA were averaged together for each patient. The weighted connectivity matrix (based on z-scores) was then converted into a binary matrix using these criteria.

Calculation of Indegree and Outdegree

To examine the network topology of the connections between brain regions, graph theoretical measures were applied to the CCEP matrices [Bassett et al., 2012; Bullmore and Sporns, 2009; Wang et al., 2011]. Specifically, indegree (the number of significant connections recorded on a BA from every other stimulating BA), outdegree (the number of significant connections measured on all BAs after stimulating a BA), and degree (the sum of indegree and outdegree) were computed using the Brain Connectivity Toolbox [Rubinov and Sporns, 2010].

Indegree and outdegree were calculated two ways. First, we looked at the single electrode level and second, at the Brodmann's area or group level. On single electrode level for indegree, we calculated every connection to a node (single electrode) from all other electrodes which were stimulated, and then divided the number with the stimulations actually performed (possible maximum number of connections) to reduce variability due to different electrode configurations and stimulation trials. For outdegree on the single electrode level, we calculated the number of outgoing connections from every node, which was also normalized with the possible maximum number of connections (e.g., the total number of recording electrodes minus the two stimulated electrodes).

To examine indegree and outdegree at the BA level, we first averaged together all the connections from the electrodes, which were placed within the same Brodmann's area on a single patient level and took every connection where the z-score exceeded a threshold of 3SD. Then we grouped
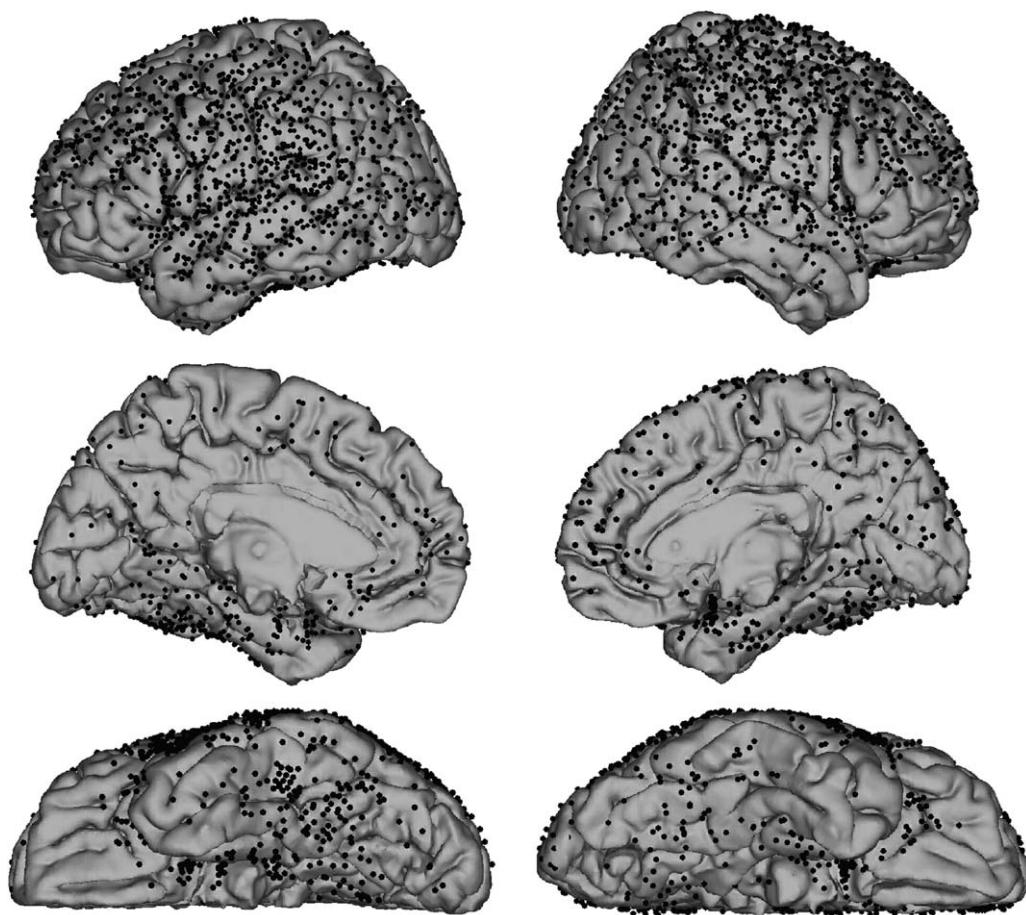
Figure 1.

Composite of electrodes implanted in 25 patients. Electrodes are shown as black dots on the standard MNI152 brain.

all the BA's of all the patients together to see the grand mean average of connections, excluding all connections which were only present in 10% of the patients, to exclude inconsistent under represented connections. Graph theory measures were normalized such that the sum of the indegree, degree, and outdegree of all stimulation sites for each patient was divided with the possible stimulations for indegree and the possible recording BAs for outdegree to reduce interindividual variability. Plots of the graph theoretical measures were created using custom scripts (MATLAB, Natick, MA).

RESULTS

Sampling of Areas

Overall, BAs localized on the convexity of the brain—including primary motor and sensory cortex, temporal lobe, and the majority of the frontal and parietal lobes—were densely covered with electrodes. Areas including the occipital pole, paracentral lobule, anterior portion of the cingulum, supplementary motor area (SMA), and the temporobasal and medial surfaces were also sampled. The insula and more caudal regions of the medial surface (i.e., PCC) were typically not sampled in most subjects (Fig. 1 and Table II).

Evoked Potentials Demonstrate Reliable Cortical Connectivity

We recorded consistent and statistically significant CCEPs in each of 25 patients implanted with subdural electrodes. An example of the thresholding process to define CCEP connections is shown in Figure 2. By these criteria (N1 and N2 peaks exceeding 3SD of the baseline), 36% (1,012/2,505) of N1 and 60% of N2 connections were significant. The time delay from the stimulation artifact for the N1 peak ranged from 10.0 to 49.5 ms (median: 21.2
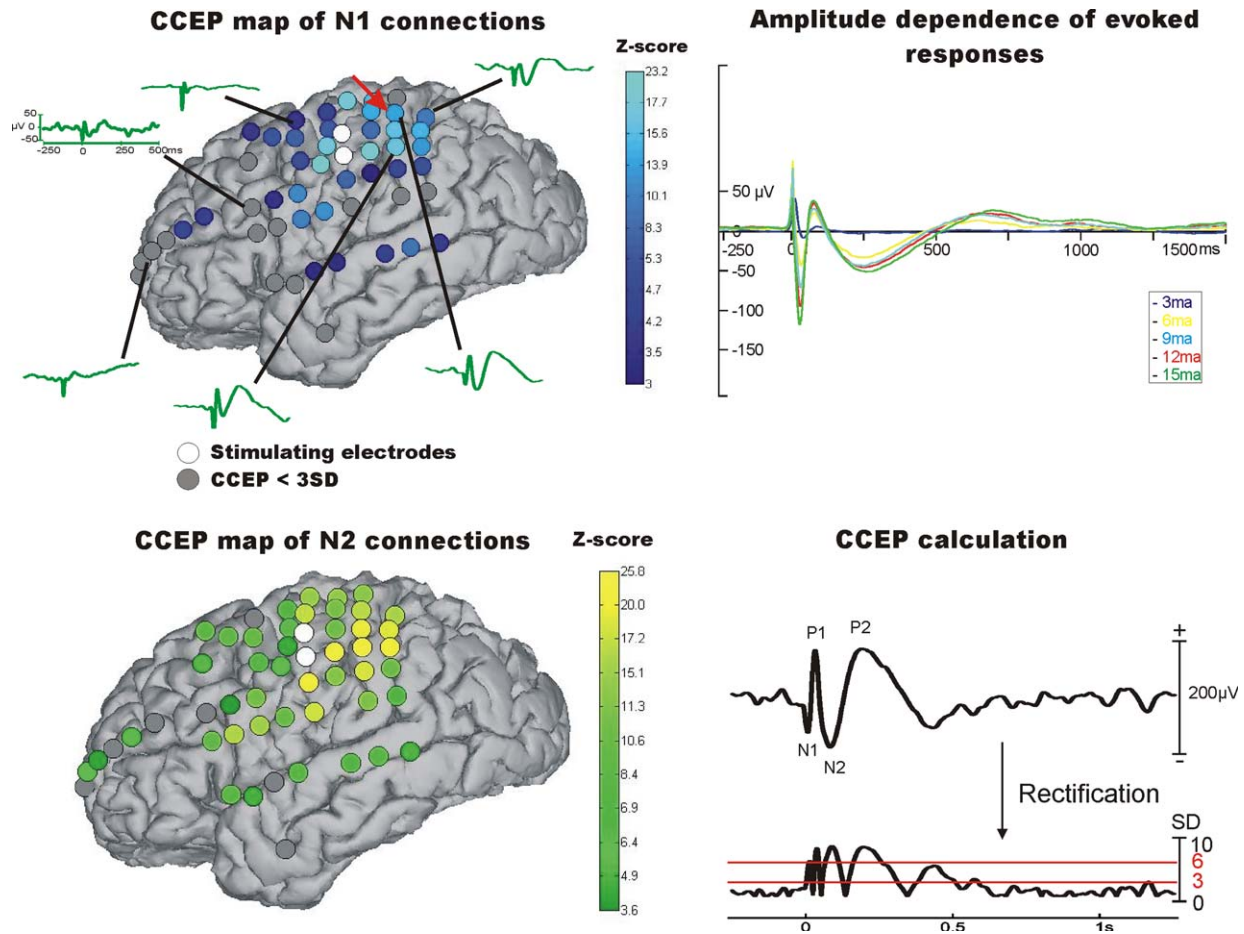
Figure 2.

CCEP connectivity: 3D reconstruction of preoperative MRI in one patient displaying the implanted electrodes snapped to the cortical surface. Circles in white are the electrodes being stimulated. Upper left image shows the CCEP z-scores of the electrodes (>3 SD) for the N1 peak. Lower left image shows the CCEP z-scores of the electrodes (>3 SD) for the N2 peak. Right upper panel displays the evoked CCEPs after stimulation of the same electrode contacts with different amplitudes (Parameters: 0.5 Hz, 0.2 ms, and 3-6-9-12-15 mA). Lower right panel depicts the calculation of significant CCEPs using full wave rectification and z-score calculation based on the prestimulus baseline. Red arrow points to the electrode (Gd55) used for demonstration of CCEP calculation.

ms) and 50.3 to 499.5 ms (median: 167.0 ms) for the N2 peak. Stimulation at 10 mA never resulted in obvious epileptiform discharges for 1,088 stimulation sites that were performed outside the epileptogenic zone.

To account for the different CCEP field distributions derived from the same stimulation site using multiple series of stimulation, we computed the intrasubject reliability based on CCEP mapping sessions performed on multiple days in a single patient. CCEP maps recorded on 3 different days within a period of 5 days demonstrated >70% similarity for N1 (70% between day 1 and 4, 71% between day 1 and 5, and 74% between day 4 and 5) and over 75% similarity for N2 (day 1 and 4: 75%, day 1 and 5: 76%, and day 4 and 5: 77%).

Evoked Potentials Demonstrate Asymmetry Across Distributed Networks

In general, CCEP connections were often found to be asymmetric (one CCEP connection was stronger than the opposing CCEP connection) based on amplitude criteria. Figure 3 depicts the asymmetry of N1 connections (if in one direction the amplitude exceeded 3SD) with 81% of connections showing a >50% difference and 88% showing a >30% difference in z-scores between directions. A similar profile was seen with the N2 (not shown), with 73% of connections demonstrating a >50% difference and 82% demonstrating a >30% difference in z-scores between directions.
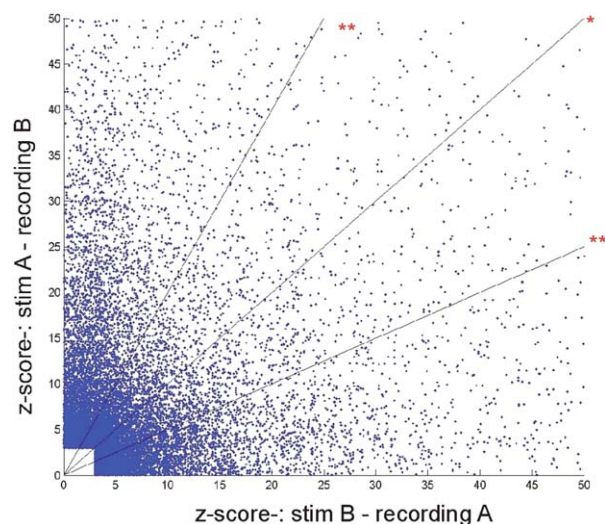
Figure 3.

Defining reciprocity on single electrode level based on N1. z-Scores of all reciprocal connections (at least one direction must fulfill a criteria of 3 SD). No linear correlation was found between z-score pairs of reciprocal connections ($R^2 = 0.011$), which corroborate the directedness of these connections. Diagonal (*) represents connections with equal amplitude, lines above and below (**) represent the threshold for 50% difference in amplitudes. [Color figure can be viewed in the online issue, which is available at wileyonlinelibrary.com.]

Effective Connectivity Decreases with Distance

Distances between electrode sites were calculated using the Euclidean distance between the midpoint of the two stimulated electrodes and the center of the recording electrode [Matsumoto et al., 2004]. This distance was always the shortest possible route between the two nodes irrespective of the convolutions of the brain. Figure 4 shows that the strength of CCEPs significantly decreased as a function of this distance between stimulating and recording electrodes ($P < 0.01$; ANOVA Kruskal–Wallis test). Of all connections that were considered significant, a larger proportion of significant connections were observed locally (<2 cm) compared to long-range (>8 cm; 67% and 27% for N1, 83% and 51% for N2, respectively). Both indegree and outdegree measures were found to be significantly higher for local interactions than long-range connections ($P < 0.01$; ANOVA Kruskal–Wallis test). Connectivity appeared to be longer range when considering the N2 component relative to the N1 component, with no observable difference between indegree and outdegree connections as a function of distance. We found significantly higher indegree and outdegree for the N2 than the N1 at every distant bin measured (N1 vs. N2, $P < 0.02$, Kolmogorov–Smirnov test).

Connectivity Analysis of the N1 Component

As the N1 is considered to reflect the afferent volley of excitation to a given area [Creutzfeldt et al., 1966; Logothe-

tis et al., 2010; Matsumoto et al., 2004], we first analyzed this component to assess connectivity. CCEP connectivity was assessed creating a connectivity matrix of z-scores for stimulated and recording BAs for each individual (e.g., Fig. 5). This yields a relative strength of connections that can be normalized by z-score for each pair of BAs tested for connectedness. To account for variability in electrode placement, indegree for each BA was normalized by dividing the number of incoming connections by the total number of connections tested. Similarly, outgoing connections from each BA were also normalized by the total number of possible connections within that specific patient.

The CCEP matrix of z-scores for each patient were averaged together to create a group-level CCEP matrix (Figs. 6 and 7). In general, the largest average z-score values for connectivity were observed between the lateral portion of the frontal, temporal, and parietal lobes, with z-scores > 12 measured between SS, BA6, BA9, BA40, Heschl's gyrus (AU), and motor cortex (M). Stimulation of BA20 revealed strong connections with broad regions of the frontal, temporal lateral and medial, parietal, and occipital lobes, while BA21 and 22 showed the strongest connections with Heschl's gyrus and only moderate connectivity with other cortical areas. Intralobar connections were strong within the occipital lobe. Stimulating V2 and V3 (V1 was not tested) showed strong intralobar connectivity and very well circumscribed strong connections to few regions including Heschl's gyrus and posterior cingulate areas for V2 and BA22 and 37 and the posterior cingulate areas (for V3; Fig. 6A for N1 with a threshold of 6SD for better specificity). A directedness of connections is evident between a number of areas. For example, stimulation of the PFC results in a larger response in the middle temporal gyrus (BA21) with an average z-score of 10.17 (N1), but the strength of the connection in the opposite direction is weaker, with stimulation in BA21 producing an average z-score of 6.25.

Consistency of connections across subjects is shown in Figure 6B. Using a 6SD criterion, stimulating BA4 or BA6 resulted in significant CCEPs at almost all recorded BAs, including each other (8/10 subjects). Both BA4 and BA6 demonstrated consistent outgoing connections to BA9 (11/11 subjects for area 6; 7/8 subjects for motor (BA4)), BA10 (9/10 subjects for area 6; 8/9 subjects for motor), BA46 (9/11 subjects for area 6; 8/10 subjects for motor), and Broca's area (7/9 subjects for area 6; 6/7 subjects for motor). In four subjects with coverage over the posterior cingulate area (a central node of the default mode network; [Fox et al., 2005] all showed responses on stimulation of the lateral frontoparietal neocortex.

Connectivity analysis of the N2

A separate z-score matrix was created for the N2 peaks to evaluate differences in connectivity during the different time frames. Figure 7 shows the corresponding analyses for the N2 component. N1 connectivity is largely mirrored
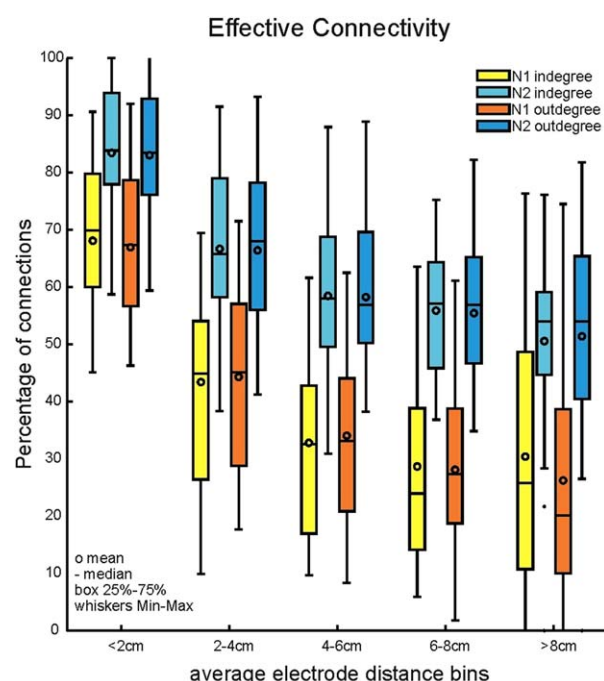
Figure 4.

The effect of distance on CCEP connectivity. The bars with lighter colors illustrate the normalized indegree as a function of distance, while the bars with darker colors show the normalized outdegree. CCEP distributions are computed in 2 cm bins. Errorbars denote minimum and maximum values. The difference between N1 and N2 is significant in every distance bin ($P < 0.05$, Kolmogorov–Smirnov) and both for indegree and outdegree. The decrease in connectivity is also significant between (<2 cm and >8 cm) the bins ($P < 0.01$; ANOVA Kruskal–Wallis test) for indegree and outdegree and for N1 and N2 as well. [Color figure can be viewed in the online issue, which is available at wileyonlinelibrary.com.]

by analysis of the N2. However, we found broader distribution of reciprocal connections with the N2, which could be the result of the yet less understood subcortico-cortical connections as indicated by Figure 7.

Analyzing the N2 component similarly to N1 revealed the central role of the motor, premotor and SS areas as well, which was very consistent across patients as seen in Figure 7B. Although there are many similarities, there are some differences as well. For example, stimulating BA20 revealed very strong connections to BA21, 22, 37, and 38 when looking at N1, with the N2 analysis although these connections were present only BA37 showed a very strong connection. When stimulating the SS cortex N2 analysis revealed very strong connections to BA7, 39, and 40, which were present when analyzing the N1 but only with lower z-scores, not indicated as a strong connection. A very well-studied connection between Broca (BR) and Wernicke (BA22) showed average or lower strength with the N1 analysis, conversely, it was shown to be very strong with the N2 measurements in both directions.

Hubs of Connectivity

Next, we localized regions exhibiting the highest degree centrality (cortical hubs) across patients. SS, motor, premotor area, and BA9/10 were identified as cortical hubs (major hubs were defined as those BAs, which exhibited total degree measures above the 95th percentile of the maximum) using both the N1 and N2 peak. When hubs were computed using the N2, they were found to be located in Broca's and Wernicke's area as well as portions of the temporal (BA21, BA22) and parietal (BA40) lobes. We do not believe this to be a sampling issue only since there are regions including BA20 and BA38, which were densely sampled in many patients, and were not found to be hubs using this analysis.

After identifying major hub regions (Fig. 8; PM, BA9, SS, M, BA10), we examined the network topology within specific functional networks. Areas with eloquent function including motor (BA4, BA6) and language areas (areas: BR and BA22) exhibited more central positions. BA20 and BA9 also occupied central positions in the network.

Directedness of BA Connections

To estimate the directedness of connectivity between BAs, a directionality index (DI) was computed as the ratio of the average z-score of the outgoing and incoming connections for each BA for both the N1 and N2 components. Accordingly, a DI greater than 1 represents relatively greater outgoing connections. If the mean strength of all CCEPs for a BA–BA connection did not exceed the significance threshold of $z = 3$ at least in one direction, the DI of this connection was not calculated as it is difficult to confidently assess directionality with nonsignificant CCEPs. BAs (30.4%) exhibited a $>50\%$ difference between indegree and outdegree connections and 43.4% of BAs showed a $>30\%$ difference using N1. Differences between indegree and outdegree for the N2 were 20.8% and 50% of BAs for $>50\%$ and $>30\%$ of areas, respectively. The distribution of DI's according to BA's is shown in Figure 9 for both the N1 and N2 components. BA20, 39, V2, showed a large out/in ratio with both analysis (N1 and N2), while the superior temporal gyrus (AU: BA41 and 42), some frontal areas (BA5, BA7) and the cingulate cortex demonstrated smaller out/in ratios with both analysis. Interestingly the amplitude differences (z-score) changed dramatically for the motor and premotor cortex between the two methods. Motor areas are showing larger amplitudes for incoming connections with the N1 analysis compared to N2, where outgoing connections evoke larger amplitude CCEPs compared to incoming connections.

DISCUSSION

We present a directional connectivity-based map of the human cortex derived from direct electrophysiological
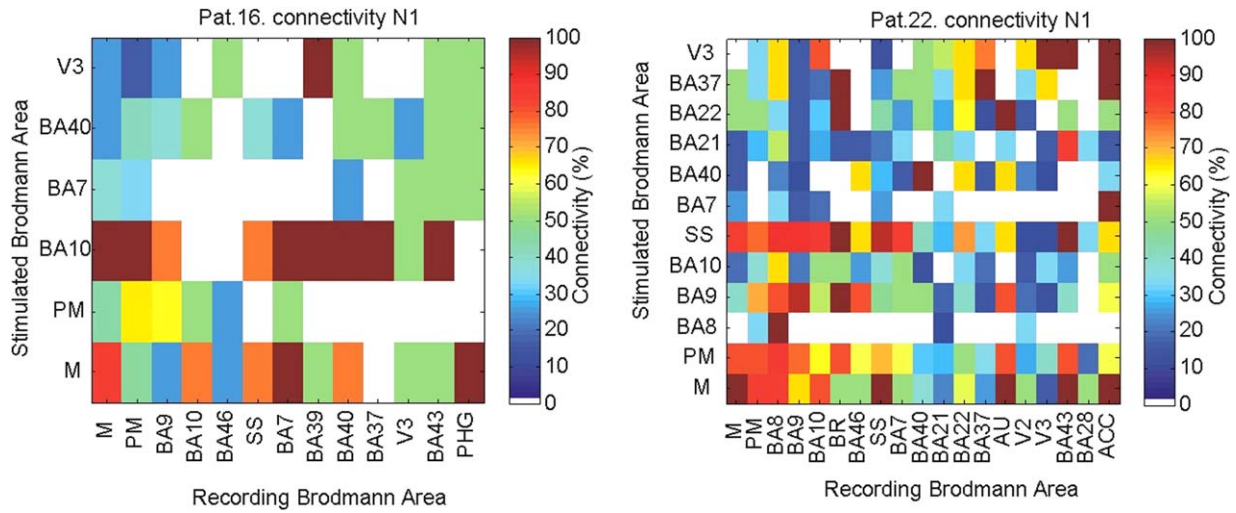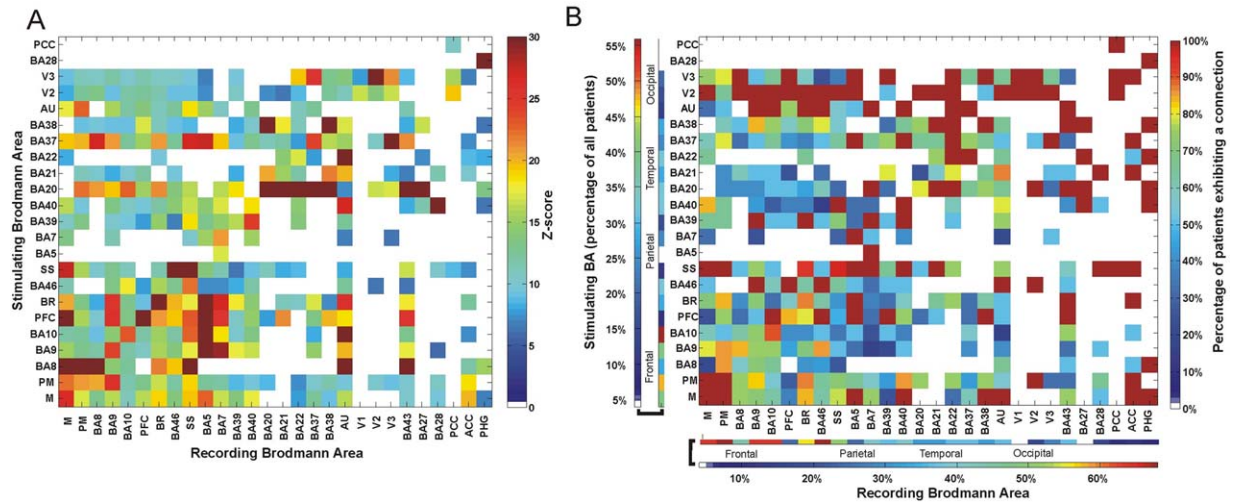
Figure 5.
Connectivity matrices for two representative patients. The matrix shows the connectivity (percentage of connections showing an amplitude of greater than 3 SD for the N1 peak vs. all possible connections) between regions covered with electrodes.

recordings of CCEPs in 25 subjects. This is a multicenter, large scale, multilobar evoked effective connectivity study in the awake, human brain using subdural electrodes, and adds to the literature using this method to explore brain connectivity [Catenoix et al., 2011; David et al., 2013; Lacruz et al., 2007; Matsumoto et al., 2004, 2007, 2012; Wilson et al., 1990]. In doing so, we aim to instruct anatomic and functional connectivity maps and other effec-

tive connectivity maps based on noninterventional methods.

Use of CCEP to Map Brain Connectivity

CCEP's have been used in the clinical setting to improve localization of the epileptogenic focus [Valentin et al.,

Figure 6.
CCEP connectivity strength and evokability for N1. **A**: Matrix shows the average z-score between and within regions using the N1 peak as the measure of connection (only z-scores above 6 are shown to highlight stronger connections). **B**: Evokability of connections between different regions and BAs. The connectivity matrix represents the percentage of patients that elicited CCEPs >6 SD between different BAs using N1.
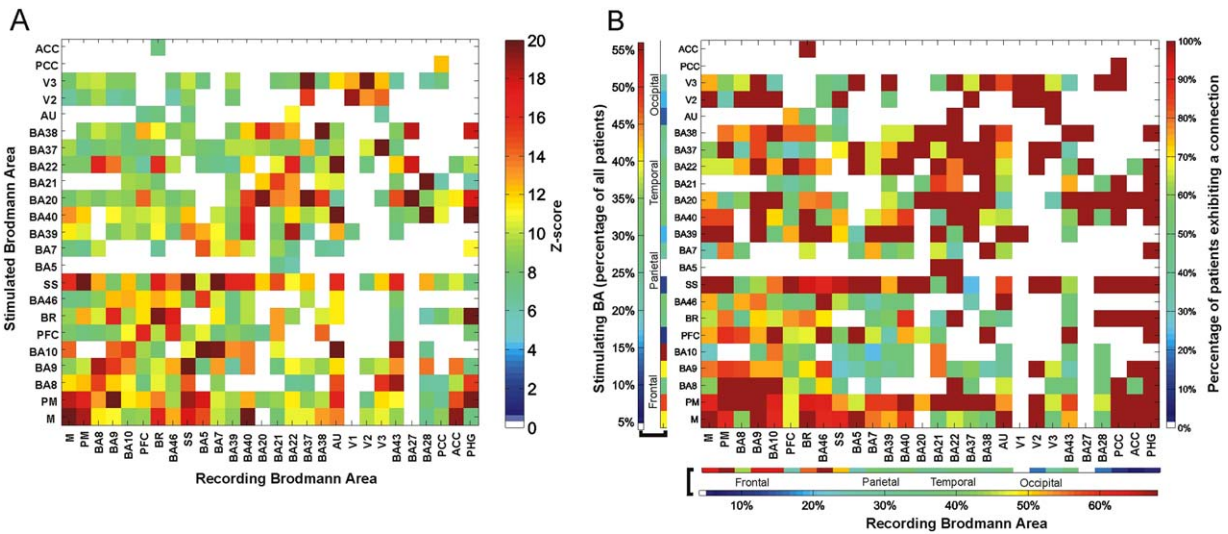
Figure 7.

CCEP connectivity strength and evokability for N2. **A**: Matrix shows the average z-score between and within regions using the N2 peak as the measure of connection (only z-scores above 6 are shown to highlight stronger connections). **B**: Evokability of connections between different regions and BAs. The connectivity matrix represents the percentage of patients that elicited CCEPs >6 SD between different BAs using N2.

2002] and to predict outcome after epilepsy surgery [Valentin et al., 2005]. Likewise, the use of CCEP to index physiological brain connectivity has been used by the same groups as a corollary measure. These measures may be obtained with minimally increased clinical resources and even less risk to subjects with a benefit at the individual subject level and beyond.

It is believed that direct electro-cortical stimulation results primarily orthodromic activation of axonal efferents due to (1) direct depolarization of pyramidal neurons and (2) indirect activation of pyramidal neurons by activation of interneurons [Jones and Wise, 1977; Matsumoto et al., 2004]. While there is likely to be some antidromic stimulation of presynaptic terminals, their relatively lesser size, density, and geometrical organization of compared to pyramidal cells makes orthodromic mechanisms more likely to contribute to the CCEP.

Some studies have focused on identifying individual functional networks, such as motor [Matsumoto et al., 2007], auditory [Brugge et al., 2003], and language [Greenlee et al., 2004; Matsumoto et al., 2004]. Heschl's gyrus stimulation results reciprocal polymorphic evoked potentials in the posterolateral superior temporal gyrus [Brugge et al., 2003]. We replicate this finding of bidirectional connectivity between BA41/42 (AU) and area 22 and also demonstrate connectivity with Broca's area and higher order extrastriate cortex (V3). Greenlee et al. [2004] demonstrated a reciprocal connection between inferior frontal gyrus (Broca's area) and orofacial motor cortex. We also

demonstrate this finding with bidirectional connections between Broca's area and motor cortex. In the present report, we add to this understanding of Broca's area by demonstrating reciprocal connectivity also with the premotor area (BA6) and by showing an indegree from BA6 and BA4 (with N2).

In the pioneering studies using this technique by Matsumoto et al. [2004], a reciprocal connection between the classical Broca's (area 44/45) and Wernicke's (area 22/40) area was shown. This finding argued against a unidirectional interpretation of the Wernicke–Geschwind model, and in support of a bidirectional influence between structures through the arcuate fasciculus or other cortico-subcortico-cortical connections. Our findings confirm Broca's area to be densely and reciprocally connected with areas that subsume the classically defined Wernicke's area, including the superior temporal gyrus (BA22) and the supramarginal gyrus (BA40). We supplement these findings by demonstrating robust outdegree connections of Broca's area to SS cortex, BA8, BA21, BA39, BA28, BA41/42, anterior cingulum, and PHG, and indegree connections from BA9, PFC, BA38, BA46, and anterior cingulum.

In another large scale study, Lacruz et al. [2007] reported a high incidence of intralobar connections using CCEP mapping. While connectivity outside the frontal and temporal lobes was not assessed, they showed a relatively greater amount of within-lobe connections, especially in the temporal lobe. Frontal lobe stimulation tended to be
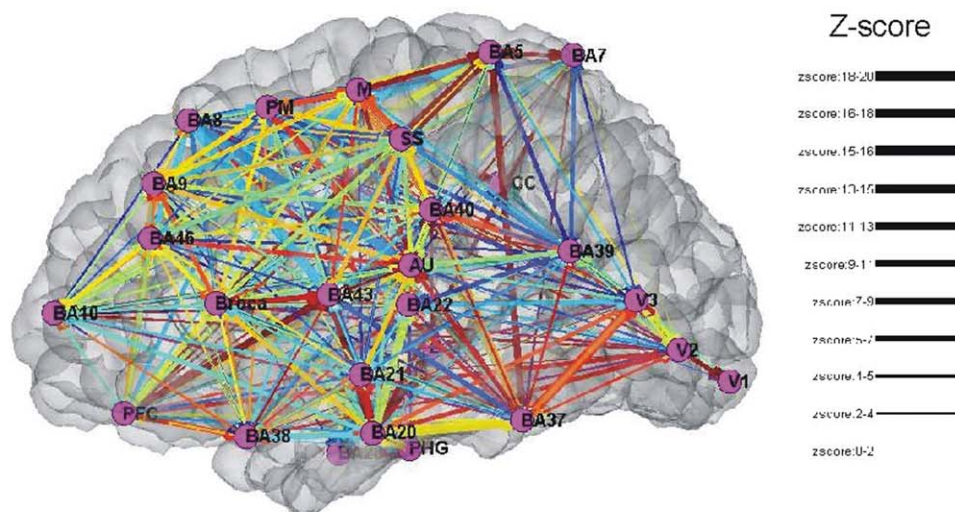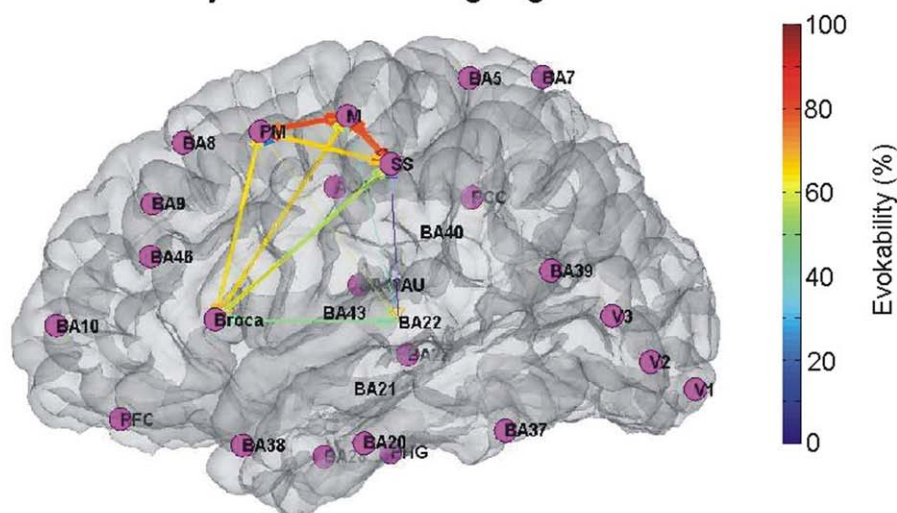
Figure 8.

Expressing directional connections between areas using the group average. **A**: Graph shows the connections between BAs, based on the connectivity matrix derived from the stimulation data. Grand mean average of all patients is shown for the N1 peak. **B**: the connections between the somatosensory and motor and the areas involved in speech and comprehension are highlighted only. The color of the edges represent the evokability (warmer colors represent higher percentage of patients exhibitng the connection), the width of the edge highlights the average z-score between the two areas.

more likely to produce responses in the contralateral frontal and ipsilateral temporal lobes. This is consistent with our results, though more so in the case of the N2 component than the N1 component. We find an exception to this general scheme in the case of BA20 in the temporal lobe, where we find high connectivity and more outdegree connections. This may be due to sampling differences between the two studies as well as parcellation differences as Lacruz et al. did not specifically look at just the inferior temporal connections.
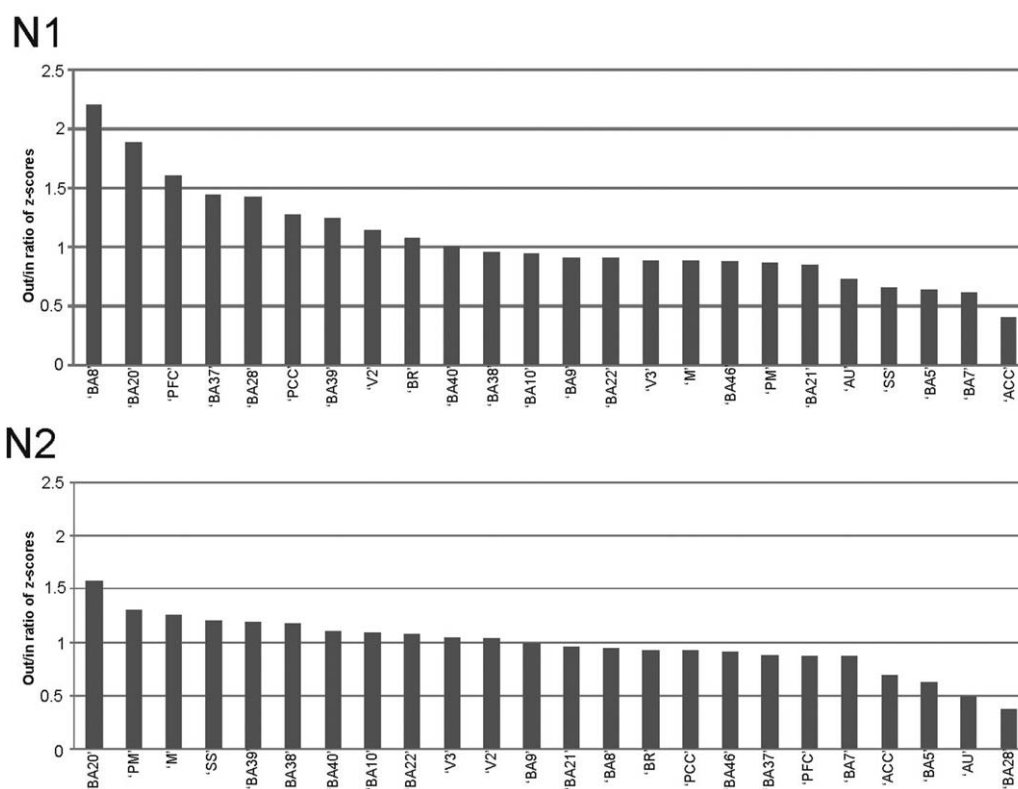
Figure 9.

Directedness of connections derived from out/in ratio of average z-scores for every region. Upper part shows the results for calculating the N1 peak of the CCEP. Lower part represents the results for using the N2 peak of the CCEP. Numbers below 1 represent regions that have higher z-scores for the incoming connections. Numbers above 1 show higher z-scores for the outgoing connections. Only regions with actual values are displayed. Temporal, somato-motor, and -sensory regions, but also parietal regions show higher values for outgoing connections and frontal and some temporal regions show higher values for incoming connections.

While the distinction between indegree and outdegree was not explored systematically, a number of CCEP studies have shown the basal temporal area to have strong connectivity to a number of other cortical areas [Koubeissi et al., 2012; Matsumoto et al., 2004; Umeoka et al., 2009]. Umeoka demonstrated a strong outdegree of the basal temporal language area (BTLA) that extended bilaterally [Umeoka et al., 2009]. Conversely, Matsumoto et al. [2004] failed to demonstrate a connection between the superior temporal gyrus (area 22) and the subtemporal areas (area 20). While we did not investigate interhemispheric connectivity, we demonstrate a high outdegree of BA20, which would include the BTLA. Clinical experience has shown stimulation of the BTLA to interfere with language function, often producing speech arrest, but its resection may not cause language deficit [Burnstine et al., 1990; Krauss et al., 1996; Lüders, 1991]. Despite the fact ESM may often produce global aphasia by stimulation of the BTLA, gamma band responses related to language often do not include the BTLA, suggesting that clinical ESM may over-estimate areas critical to function by producing interference of projections [Crone et al., 2001]. The large outdegree of BA20 would be consistent with an area that exerts great influence on other areas, but is not critical to their function. This observation highlights the importance of understanding directionality of connections for both normal function and disease.

Relationship of CCEP Mapping to Other Measures of Connectivity

The latency and amplitude of the N1 demonstrates a positive correspondence with anatomical connectivity defined by diffusion tensor imaging [Conner et al., 2011], while both the N1 and N2 time periods of the CCEP positively correlate with connectivity measures defined by resting state fMRI [Keller et al., 2011]. While a number of studies have also shown correspondence between connectivity measures based on spontaneous electrocorticography

and fMRI [He and Liu, 2008; Keller et al., 2013; Nir et al., 2008], different techniques may reveal different network topologies.

Analyses of the topology of anatomical connections in the macaque cortex reveal V4 and area 46 to demonstrate a high degree centrality [Honey et al., 2007], we do not show this finding. We would partially account for these discrepancies due to limited sampling as well as interspecies differences. Conversely, we see more posterior regions of the frontal lobe (motor and premotor cortex) to have greater centrality. Structural and functional connectivity datasets from humans reveal hubs in the precuneus and medial PFC [Gong et al., 2009]. While we find hubs in BA9 and 10 corresponding to the medial PFC, we do not find area 7 of the precuneus to exhibit high centrality. This latter difference may partially be accounted for the fact that our sampling of area 7 is largely on its lateral rather than medial surface, the latter of which appears to be the hub in structural and functional connectivity studies [Bullmore and Sporns, 2009].

Early and Late Components of the CCEP

While CCEP's may be quite variable in morphology, in most cases, they may be qualitatively described as an early sharper peak occurring between 10 and 50 ms followed by a later, slower wave from 50 to 500 ms. This was first described by Creutzfeldt [1966] in the anesthetized cat motor cortex, where single cells show an early excitatory postsynaptic potential (EPSP) followed by a later inhibitory postsynaptic potential (IPSP) in response to both thalamic and direct cortical stimulation. It is likely, and generally accepted, that the N1 component corresponds to EPSP's driven by the afferent volley and is oligosynaptic [Avoli and Gloor, 1982; Conner et al., 2011; Matsumoto et al., 2004, 2007]. It has also been suggested that the later N2 component reflects more polysynaptic relays that include cortico-cortico-cortical, cortico-thalamo-cortical, and cortico-basal ganglia-cortical pathways [Matsumoto et al., 2004]. However, in the cat's visual cortex, Logothetis et al. [2010] showed the afferent volley to generate both early and late responses, but this tended not to propagate trans-synaptically to more higher order cortical areas unless there was pharmacological disabling of IPSPs. This may imply that the N2 may be dominated by the same afferent input that drives the N1. The N2 also appears to reflect a cortical down-state followed by an up-state, a pattern that is similar to slow oscillations in slow wave sleep that engages multiple widespread brain areas in a complex regulatory process [Csercsa et al., 2010; Hangya et al., 2011]. According to this, the N1 component might be more suitable for analyzing direct cortico-cortical connections and the N2 reflects rather complex network topologies. Further studies will be required to determine the exact neural generators of these components, and while there is considerable overlap between these components, there are some differences that are apparent between the N1 and N2 connectivity profiles.

A second issue relates to the relationship of connectivity to distance. A greater degree of short range connectivity would be expected from relatively large number of local horizontal and superficial U fiber system connections compared to long-range fibers that interconnect more distant areas [Schüz and Braitenberg, 2002]. As predicted, connectivity decreases with increasing distance in both the N1 and N2 response. These findings are in accordance with general aspects of brain network organizations as revealed with functional imaging indicating a small-worldness [Rubinov and Sporns, 2010; Sporns et al., 2004; Tononi et al., 1994]. Previous studies have shown the N2 potential to have a larger spatial distribution than the N1 potential [Matsumoto et al., 2004], which we could replicate in our analysis and found significant difference in every measured distance bin ($P < 0.05$, Kolmogorov–Smirnov).

Interventional Measurements of Effective Connectivity

The ability to record direct electrophysiological measures following the injection of current provides the most direct technique to measure effective cortico-cortical connectivity in the awake human brain. Furthermore, in this technique, we are able to measure the directional influences on inter-regional relationships. We show here that cortico-cortical interactions are not always symmetrically reciprocal, and yet the majority of techniques used to measure large-scale connectivity (DTI, RSFC) assume a nondirectional connectivity.

Noninterventional analytic approaches to infer causality have included the use of Granger analysis applied towards fMRI [David, 2007; Goebel et al., 2003] and EEG [Brovelli et al., 2004; Nedungadi et al., 2009]. Accordingly, area A Granger causes activity in another area B if the activity in area A better predicts the future activity of area B than area B's past. While refinements including transfer entropy analysis and dynamic causal modeling may improve the application of noninterventional methods [Friston et al., 2003], these methods can only reveal statistical likelihoods of causal interactions. Conversely, interventional approaches are possible in limited circumstances as in the clinical situation of patients undergoing invasive electrode monitoring for epilepsy or by combining expensive noninvasive methods with lesser spatial accuracy such as TMS and MEG. However, this limited circumstance can provide a standard by which noninterventional implied methods of causality may be examined.

Limitations

A major limitation of this study involves the fact that implanted electrodes sample a limited and variable proportion of the surface of the cerebral cortex. Furthermore, while

the lateral aspects of the hemispheres are well-sampled, the medial and inferior aspects are sampled less, and there is no direct recording from the depth of the sulci. By combining databases using the alternative stereo-EEG approach [David et al., 2013], it would be possible to include more sulcal and interhemispheric structures. Noninvasive neuroimaging methods have the advantage of greater sampling and may be used to supplement the current measures by applying noninvasive causality measures that may be instructed by invasive measures.

We chose a Brodmann's scheme supplemented by functional measures to parcellate areas. Other parcellation schemes, for example, using Freesurfer, may be used as well and may provide alternative graphical maps. In fact, apparent connectivity would be likely to depend on the parcellation scheme that is used. Stimulation of cortical areas next to each other within the same BA may result in different CCEP distribution, averaging these results together might reduce the variability and directedness of connections from a single BA. Since our goal was to create a global connectivity map of the brain, we focused on large cortical areas and used some degree of summation to be able to combine results from more than one subject. As DTI tractography has been shown to correlate with the N1 component [Conner et al., 2011], this may provide an approach to parcellating areas based on individual anatomy. Data-driven parcellation methods, such as those used in the imaging literature [Craddock et al., 2012] may ultimately be the best approach to account for clustering of connections that may exist only at an individual region. Matsumoto et al. [2007] used such a data driven approach based on amplitude and N1 latency of CCEP subfields. This represents an alternative means to examine the specific issues such as directionality, effect of distance, and graph theory metrics at the individual electrode or set of electrodes level. The future holds promise for applying these analyses into larger databases of subjects with CCEP mapping to identify them consistently and test data-driven clustering models. This would be facilitated by a multi-institutional collaboration to create databases of larger numbers of subjects with greater overall sampling of brain areas.

It should also be considered that any measure of directedness is also dependent on areas sampled. Apparent connectivity will be dependent on to what degree the sampled regions are connected. For example, if in a certain case, a larger number of areas with low connectivity are measured, the overall connectivity will appear lower. While this is clearly an important consideration regarding interpretation of the present results, we do see similar connections with respect to BAs and their directionality across subjects despite different implantation schemes. A greater sampling with more subjects should reduce this element of bias, again advocating for an effort to increase and combine databases.

Deriving conclusions regarding normal physiological processes from pathological brains is another potential limitation. We aimed to exclude all of the areas which had overt cortical abnormality or it was involved in ictal activity. However, it remains possible that some component of our observations may be biased by the pathophysiology of epilepsy. Since epilepsy is a very heterogeneous disease and the patients included in the study have various etiologies behind the epileptic manifestations, this could also rule out a common factor which would influence our results [David et al., 2013].

Future Directions

The use of CCEP mapping to describe a functional tractography has been advocated in prior reports [David et al., 2013; Matsumoto et al., 2007]. While the sampling of each subject's brain by electrodes is somewhat sparse, a more comprehensive map may be possible by combining results of multiple patients and across centers. The grids and strips approach, as in the present study, provides a larger view that is limited to cortical areas located on the brain convexity. Stereoelectroencephalography (SEEG), in which arrays penetrating depth electrodes are placed directly into the brain parenchyma provide sparser sampling, but have the advantage of sampling areas in the cortical sulci. Combination of results derived from SEEG investigations and subdural electrodes, using strict protocols, could reveal the connectivity of regions not typically sampled with only using one of the techniques. For example, the insula is very difficult to record from using subdural electrodes, but it is routinely recorded from using SEEG. This combination could reveal the connections from and to the insular cortex to those regions which are typically not covered with SEEG electrodes, such as the parietal or occipital lobes.

While cortical stimulation is performed routinely at many epilepsy centers, SPES for CCEP mapping is not. Evidence for improved clinical outcomes [David et al., 2010; Valentin et al., 2005] as well as minimal effort and patient risk have resulted in more and more centers performing these protocols for clinical indications. To do so, it will be important to establish protocols by which to perform CCEP mapping (e.g., stimulation parameters, analysis of signals) and means to group findings using parcellation schemes (e.g., MNI space, Freesurfer) or data-driven methods to cluster data [Craddock et al., 2012]. By doing so, a more comprehensive description of brain connectivity will result by combining databases from multiple centers as has been the case for functional connectivity using resting fMRI [Biswal et al., 2010; Mennes et al., 2013]. As we demonstrate here, the ease of combining databases from two different centers, adding more data from other centers will surely improve the robustness of findings. We would hope that a similar initiative may be undertaken for connectivity databases based on fMRI and electrocorticography.

The possibility of measuring direct cortical signals after well-localized stimulation of the cortex is a unique

opportunity to reveal networks involved in various brain functions. This method can create the basis of future investigations related to specific brain networks and also validate functional neuroimaging data. Future research may be performed to define specific inter- and intralobar as well as the interhemispheric connectivity of the brain. This method may also be used to localize pathological networks, which relate to epilepsy, movement disorders, as well as a host of neuropsychiatric diseases.

REFERENCES

Avoli M, Gloor P (1982): Interaction of cortex and thalamus in spike and wave discharges of feline generalized penicillin epilepsy. Exp Neurol 76:196–217.

Bassett DS, Nelson BG, Mueller BA, Camchong J, Lim KO (2012): Altered resting state complexity in schizophrenia. Neuroimage 59:2196–2207.

Biswal BB, Mennes M, Zuo XN, Gohel S, Kelly C, Smith SM, Beckmann CF, Adelstein JS, Buckner RL, Colcombe S and others (2010): Toward discovery science of human brain function. Proc Natl Acad Sci USA 107:4734–4739.

Brovelli A, Ding M, Ledberg A, Chen Y, Nakamura R, Bressler SL (2004): Beta oscillations in a large-scale sensorimotor cortical network: directional influences revealed by Granger causality. Proc Natl Acad Sci USA 101:9849–9854.

Brugge JF, Volkov IO, Garell PC, Reale RA, Howard MA III (2003): Functional connections between auditory cortex on Heschl's gyrus and on the lateral superior temporal gyrus in humans. J Neurophysiol 90:3750–3763.

Bullmore E, Sporns O (2009): Complex brain networks: graph theoretical analysis of structural and functional systems. Nat Rev Neurosci 10:186–198.

Burnstine TH, Lesser RP, Hart J Jr, Uematsu S, Zinreich SJ, Krauss GL, Fisher RS, Vining EP, Gordon B (1990): Characterization of the basal temporal language area in patients with left temporal lobe epilepsy. Neurology 40:966–970.

Cash SS, Halgren E, Dehghani N, Rossetti AO, Thesen T, Wang C, Devinsky O, Kuzniecky R, Doyle W, Madsen JR, Bromfield E, Eross L, Halász P, Karmos G, Csercsa R, Wittner L, Ulbert I. (2009): The human K-complex represents an isolated cortical down-state. Science 324:1084–1087.

Catenoix H, Magnin M, Guenot M, Isnard J, Mauguiere F, Ryvlin P (2005): Hippocampal-orbitofrontal connectivity in human: an electrical stimulation study. Clin Neurophysiol 116:1779–1784.

Catenoix H, Magnin M, Mauguiere F, Ryvlin P (2011): Evoked potential study of hippocampal efferent projections in the human brain. Clin Neurophysiol 122:2488–2497.

Conner CR, Ellmore TM, Disano MA, Pieters TA, Potter AW, Tandon N (2011): Anatomic and electro-physiologic connectivity of the language system: A combined DTI-CCEP study. Comput Biol Med 41:1100–1109.

Conturo TE, Lori NF, Cull TS, Akbudak E, Snyder AZ, Shimony JS, McKinstry RC, Burton H, Raichle ME (1999): Tracking neuronal fiber pathways in the living human brain. Proc Natl Acad Sci USA 96:10422–10427.

Craddock RC, James GA, Holtzheimer PE, 3rd, Hu XP, Mayberg HS (2012): A whole brain fMRI atlas generated via spatially constrained spectral clustering. Hum Brain Mapp 33:1914–1928.

Creutzfeldt OD, Watanabe S, Lux HD (1966): Relations between EEG phenomena and potentials of single cortical cells. I. Evoked responses after thalamic and erpicortical stimulation. Electroencephalogr Clin Neurophysiol 20:1–18.

Crone NE, Hao L, Hart J, Jr., Boatman D, Lesser RP, Irizarry R, Gordon B (2001): Electrocorticographic gamma activity during word production in spoken and sign language. Neurology 57:2045–2053.

Csercsa R, Dombovari B, Fabo D, Wittner L, Eross L, Entz L, Solyom A, Rasonyi G, Szucs A, Kelemen A, Jakus R, Juhos V, Grand L, Magony A, Halász P, Freund TF, Maglóczky Z, Cash SS, Papp L, Karmos G, Halgren E, Ulbert I (2010): Laminar analysis of slow wave activity in humans. Brain 133:2814–2829.

Dale AM, Fischl B, Sereno MI (1999): Cortical surface-based analysis. I. Segmentation and surface reconstruction. Neuroimage 9:179–194.

David O (2007): Dynamic causal models and autopoietic systems. Biol Res 40:487–502.

David O, Bastin J, Chabardes S, Minotti L, Kahane P (2010): Studying network mechanisms using intracranial stimulation in epileptic patients. Front Syst Neurosci 4:148.

David O, Job AS, De Palma L, Hoffmann D, Minotti L, Kahane P (2013): Probabilistic functional tractography of the human cortex. Neuroimage 80:307–317.

Duncan JS, Papademetris X, Yang J, Jackowski M, Zeng X, Staib LH (2004): Geometric strategies for neuroanatomic analysis from MRI. Neuroimage 23 Suppl 1:S34–S45.

Dykstra AR, Chan AM, Quinn BT, Zepeda R, Keller CJ, Cormier J, Madsen JR, Eskandar EN, Cash SS (2011): Individualized localization and cortical surface-based registration of intracranial electrodes. Neuroimage 59:3563–3570.

Enatsu R, Matsumoto R, Piao Z, O'Connor T, Horning K, Burgess RC, Bulacio J, Bingaman W, Nair DR (2013): Cortical negative motor network in comparison with sensorimotor network: A cortico-cortical evoked potential study. Cortex 49:2080–2096.

Entz L, Fabo D, Eross L, Halasz P, Wittner L, Karmos G, Ulbert I (2009): Single Pulse Cortical Electrical Stimulation Induced Slow Oscillation In Different Vigilance States in Epileptic Patients. Budapest, Hungary. p 93.

Eross L, Bago AG, Entz L, Fabo D, Halasz P, Balogh A, Fedorcsak I (2009): Neuronavigation and fluoroscopy-assisted subdural strip electrode positioning: a simple method to increase intraoperative accuracy of strip localization in epilepsy surgery. J Neurosurg 110:327–331.

Felleman DJ, Van Essen DC (1991): Distributed hierarchical processing in the primate cerebral cortex. Cereb Cortex 1:1–47.

Fox MD, Snyder AZ, Vincent JL, Corbetta M, Van Essen DC, Raichle ME (2005): The human brain is intrinsically organized into dynamic, anticorrelated functional networks. Proc Natl Acad Sci USA 102:9673–9678.

Friston KJ, Harrison L, Penny W (2003): Dynamic causal modelling. Neuroimage 19:1273–1302.

Goebel R, Roebroeck A, Kim DS, Formisano E (2003): Investigating directed cortical interactions in time-resolved fMRI data using vector autoregressive modeling and Granger causality mapping. Magn Reson Imaging 21:1251–1261.

Goldring S, Harding GW, Gregorie EM (1994): Distinctive electrophysiological characteristics of functionally discrete brain areas: a tenable approach to functional localization. J Neurosurg 80:701–709.

Gong G, He Y, Concha L, Lebel C, Gross DW, Evans AC, Beaulieu C (2009): Mapping anatomical connectivity patterns of human cerebral cortex using in vivo diffusion tensor imaging tractography. Cereb Cortex 19:524–536.

Gordon B, Lesser RP, Rance NE, Hart J, Jr., Webber R, Uematsu S, Fisher RS (1990): Parameters for direct cortical electrical stimulation in the human: histopathologic confirmation. Electroencephalogr Clin Neurophysiol 75:371–377.

Greenlee JD, Oya H, Kawasaki H, Volkov IO, Kaufman OP, Kovach C, Howard MA, Brugge JF (2004): A functional connection between inferior frontal gyrus and orofacial motor cortex in human. J Neurophysiol 92:1153–1164.

Hagmann P, Cammoun L, Gigandet X, Meuli R, Honey CJ, Wedeen VJ, Sporns O (2008): Mapping the structural core of human cerebral cortex. PLoS Biol 6:e159.

Hamberger MJ (2007): Cortical language mapping in epilepsy: A critical review. Neuropsychol Rev 17:477–489.

Hangya B, Tihanyi BT, Entz L, Fabo D, Eross L, Wittner L, Jakus R, Varga V, Freund TF, Ulbert I (2011): Complex propagation patterns characterize human cortical activity during slow-wave sleep. J Neurosci 31:8770–8779.

He B, Liu Z (2008): Multimodal functional neuroimaging: integrating functional MRI and EEG/MEG. IEEE Rev Biomed Eng 1:23–40.

Honey CJ, Kotter R, Breakspear M, Sporns O (2007): Network structure of cerebral cortex shapes functional connectivity on multiple time scales. Proc Natl Acad Sci USA 104:10240–10245.

Jenkinson M, Smith S (2001): A global optimisation method for robust affine registration of brain images. Med Image Anal 5:143–156.

Jones EG, Wise SP (1977): Size, laminar and columnar distribution of efferent cells in the sensory-motor cortex of monkeys. J Comp Neurol 175:391–438.

Keller CJ, Bickel S, Entz L, Ulbert I, Milham MP, Kelly C, Mehta AD (2011): Intrinsic functional architecture predicts electrically evoked responses in the human brain. Proc Natl Acad Sci U S A 108:10308–10313.

Keller CJ, Bickel S, Honey C, Groppe D, Entz L, Craddock R, Lado F, Kelly C, Milham MP, Mehta AD (2013): Neurophysiological investigation of spontaneous correlated and anticorrelated fluctuations of the BOLD signal. Journal of Neuroscience in press.

Koubeissi MZ, Lesser RP, Sinai A, Gaillard WD, Franaszczuk PJ, Crone NE (2012): Connectivity between perisylvian and bilateral basal temporal cortices. Cereb Cortex 22:918–925.

Krauss GL, Fisher R, Plate C, Hart J, Uematsu S, Gordon B, Lesser RP (1996): Cognitive effects of resecting basal temporal language areas. Epilepsia 37:476–483.

Lacruz ME, Garcia Seoane JJ, Valentin A, Selway R, Alarcon G (2007): Frontal and temporal functional connections of the living human brain. Eur J Neurosci 26:1357–1370.

Logothetis NK, Augath M, Murayama Y, Rauch A, Sultan F, Goense J, Oeltermann A, Merkle H (2010): The effects of electrical microstimulation on cortical signal propagation. Nat Neurosci 13:1283–1291.

Lüders HO (1991): Epilepsy Surgery. New York: Raven Press.

Massimini M, Ferrarelli F, Huber R, Esser SK, Singh H, Tononi G (2005): Breakdown of cortical effective connectivity during sleep. Science 309:2228–2232.

Matsumoto R, Nair DR, LaPresto E, Najm I, Bingaman W, Shibasaki H, Luders HO (2004): Functional connectivity in the human language system: a cortico-cortical evoked potential study. Brain 127(Pt 10):2316–2330.

Matsumoto R, Nair DR, LaPresto E, Bingaman W, Shibasaki H, Luders HO (2007): Functional connectivity in human cortical motor system: a cortico-cortical evoked potential study. Brain 130(Pt 1):181–197.

Matsumoto R, Nair DR, Ikeda A, Fumuro T, Lapresto E, Mikuni N, Bingaman W, Miyamoto S, Fukuyama H, Takahashi R, Najm I, Shibasaki H, Lüders HO. (2012): Parieto-frontal network in humans studied by cortico-cortical evoked potential. Hum Brain Mapp 33:2856–2872.

McIntosh AR, Gonzalez-Lima F (1994): Structural equation modeling and its application to network analysis in functional brain imaging. Human Brain Mapping 2:2–22.

Mennes M, Biswal BB, Castellanos FX, Milham MP (2013): Making data sharing work: the FCP/INDI experience. Neuroimage 82:683–691.

Nedungadi AG, Rangarajan G, Jain N, Ding M (2009): Analyzing multiple spike trains with nonparametric Granger causality. J Comput Neurosci 27:55–64.

Nir Y, Mukamel R, Dinstein I, Privman E, Harel M, Fisch L, Gelbard-Sagiv H, Kipervasser S, Andelman F, Neufeld MY, Kramer U, Arieli A, Fried I, Malach R. (2008): Interhemispheric correlations of slow spontaneous neuronal fluctuations revealed in human sensory cortex. Nat Neurosci 11:1100–1108.

Purpura DP, Pool JL, Ransohoff J, Frumin MJ, Housepian EM (1957): Observations on evoked dendritic potentials of human cortex. Electroencephalogr Clin Neurophysiol 9:453–459.

Rosenberg DS, Mauguiere F, Catenoix H, Faillenot I, Magnin M (2009): Reciprocal thalamocortical connectivity of the medial pulvinar: a depth stimulation and evoked potential study in human brain. Cereb Cortex 19:1462–1473.

Rubinov M, Sporns O (2010): Complex network measures of brain connectivity: uses and interpretations. Neuroimage 52:1059–1069.

Schüz A, Braitenberg V (2002): The human cortical white matter: Quantitative aspects of cortico-cortical long-range connectivity. In: Schüz A, Miller R, editors. Cortical Areas: Unity and Diversity. London, New York: Taylor and Francis.

Smith JF, Pillai A, Chen K, Horwitz B (2011): Effective connectivity modeling for fMRI: Six issues and possible solutions using linear dynamic systems. Front Syst Neurosci 5:104.

Smith SM (2002): Fast robust automated brain extraction. Hum Brain Mapp 17:143–155.

Sporns O, Chialvo DR, Kaiser M, Hilgetag CC (2004): Organization, development and function of complex brain networks. Trends Cogn Sci 8:418–425.

Steriade M (2003): The corticothalamic system in sleep. Front Biosci 8:d878–d899.

Tononi G, Sporns O, Edelman GM (1994): A measure for brain complexity: relating functional segregation and integration in the nervous system. Proc Natl Acad Sci USA 91:5033–5037.

Umeoka S, Terada K, Baba K, Usui K, Matsuda K, Tottori T, Usui N, Nakamura F, Inoue Y, Fujiwara T, Mihara T. (2009): Neural connection between bilateral basal temporal regions: cortico-cortical evoked potential analysis in patients with temporal lobe epilepsy. Neurosurgery 64:847–855; discussion 855.

Valentin A, Anderson M, Alarcon G, Seoane JJ, Selway R, Binnie CD, Polkey CE. (2002): Responses to single pulse electrical stimulation identify epileptogenesis in the human brain in vivo. Brain 125(Pt 8):1709–1718.

Valentin A, Alarcon G, Honavar M, Garcia Seoane JJ, Selway RP, Polkey CE, Binnie CD (2005): Single pulse electrical stimulation for identification of structural abnormalities and prediction of seizure outcome after epilepsy surgery: a prospective study. Lancet Neurol 4:718–726.

Vincent JL, Patel GH, Fox MD, Snyder AZ, Baker JT, Van Essen DC, Zempel JM, Snyder LH, Corbetta M, Raichle ME (2007): Intrinsic functional architecture in the anaesthetized monkey brain. Nature 447:83–86.

Wang JH, Zuo XN, Gohel S, Milham MP, Biswal BB, He Y (2011): Graph theoretical analysis of functional brain networks: test-retest evaluation on short- and long-term resting-state functional MRI data. PLoS One 6:e21976.

Wilson CL, Isokawa M, Babb TL, Crandall PH (1990): Functional connections in the human temporal lobe. I. Analysis of limbic system pathways using neuronal responses evoked by electrical stimulation. Exp Brain Res 82:279–292.

Yamao Y, Matsumoto R, Kunieda T, Arakawa Y, Kobayashi K, Usami K, Shibata S, Kikuchi T, Sawamoto N, Mikuni N, Ikeda A, Fukuyama H, Miyamoto S (2014): Intraoperative dorsal language network mapping by using single-pulse electrical stimulation. Hum Brain Mapp.